NACA RM H54L27

NACA



# RESEARCH MEMORANDUM

## WING-LOAD MEASUREMENTS AT SUPERSONIC SPEEDS OF THE DOUGLAS D-558-II RESEARCH AIRPLANE

By Glenn H. Robinson, George E. Cothren, Jr., and Chris Pembo

High-Speed Flight Station
Edwards, Calif.





NATIONAL ADVISORY COMMITTEE
FOR AERONAUTICS

WASHINGTON

March 30, 1955

NATIONAL ADVISORY COMMITTEE FOR AERONAUTICS

RESEARCH MEMORANDUM

# WING-LOAD MEASUREMENTS AT SUPERSONIC SPEEDS OF THE DOUGLAS D-558-II RESEARCH AIRPLANE

By Glenn H. Robinson, George E. Cothren, Jr., and Chris Pembo

## SUMMARY

Flight measurements of the aerodynamic wing loads on the D-558-II airplane have been made in the Mach number range from 1.0 to 2.0.

Nonlinear wing-panel characteristics occurred with variations in angle of attack. These nonlinear characteristics were apparent primarily at the lower supersonic speeds. At these speeds a reduction in the slope of the wing-panel normal-force curve occurred, and the wing-panel center of pressure moved inboard and forward at the higher lifts. At the higher Mach numbers where a smaller lift range was investigated small nonlinearities were apparent in the pitching-moment curves.

For comparable lift ranges the changes in the wing characteristics with Mach number were small.

## INTRODUCTION

As a part of the cooperative Air Force—Navy—NACA high-speed flight research program the Douglas D-558-II research airplane has been used in an exploratory program to investigate the lift and Mach number capabilities of the airplane. These tests were conducted over a Mach number range from 1.0 to 2.0 at altitudes from 40,000 to 70,000 feet. Measurements of the wing loads were made during these tests in dives and accelerated maneuvers by strain-gage methods. The results of the wing-load measurements are presented herein.

## SYMBOLS

| | |
|---|---|
| $BM_W$ | wing-panel bending moment about the gage station, ft-lb |
| $b_W/2$ | span of right wing panel outboard of gage station, ft |
| $C_{B_W}$ | wing-panel bending-moment coefficient, $\frac{BM_W}{q \frac{S_W}{2} \frac{b_W}{2}}$ |
| $C_{m_{\bar{c}_W/4}}$ | wing-panel pitching-moment coefficient about the quarter chord of the wing panel M.A.C., $\frac{M_W}{q \frac{S_W}{2} \bar{c}_W}$ |
| $C_{N_A}$ | airplane normal-force coefficient, $nW/qS$ |
| $C_{N_{A_\alpha}}$ | airplane normal-force-coefficient slope, per deg |
| $C_{N_W}$ | wing-panel normal-force coefficient, $\frac{L_W}{q \frac{S_W}{2}}$ |
| $C_{N_{W_\alpha}}$ | wing-panel normal-force-coefficient slope, per deg |
| $c_W$ | streamwise chord at any section along wing-panel span, ft |
| $\bar{c}_W$, M.A.C.$_W$ | mean aerodynamic chord of wing panel, $\frac{\int_0^{b_W/2} c_W^2 dy}{\int_0^{b_W/2} c_W \, dy}$ |
| $g$ | acceleration due to gravity, ft/sec$^2$ |
| $h_p$ | pressure altitude, ft |
| $L_W$ | aerodynamic wing-panel load, lb |
| $M$ | Mach number |

| | |
|---|---|
| $M_W$ | wing-panel pitching moment, ft-lb |
| n | airplane normal acceleration, g units |
| q | dynamic pressure, $\rho V^2/2$, lb/sq ft |
| S | area of wing bounded by leading edge and trailing edge extended to the airplane line of symmetry, sq ft |
| $S_W/2$ | wing-panel area outboard of right wing gage station, sq ft |
| V | free-stream velocity, ft/sec |
| W | airplane gross weight, lb |
| $x_{cp}$ | wing-panel chordwise center of pressure, percent $\bar{c}_W$ |
| $y_{cp}$ | wing-panel spanwise center of pressure, percent $b_W/2$ |
| y | lateral displacement, ft |
| $\alpha_i$ | indicated airplane angle of attack, deg |
| $\rho$ | mass density of air, slugs/ft$^3$ |

## AIRPLANE

The airplane used for these tests was the D-558-II airplane modified for supersonic flight by conversion to an all-rocket airplane. The airplane has a wing sweepback of 35° measured at the 0.30 chord of the unswept wing panel, and has a streamwise wing thickness of 8.7 percent at the root and 9.6 percent at the tip. The airplane has leading-edge slats which were locked closed during these tests and had a partial chord fence installed at 36 percent of the wing semispan for a portion of these tests. Table I presents pertinent airplane physical characteristics and figure 1 presents a three-view drawing of the airplane. Photographs of the airplane are shown in figure 2.

## INSTRUMENTATION AND ACCURACY

Standard NACA recording instruments are installed in the airplane to measure the following quantities pertinent to this investigation:

Airspeed
Altitude
Angle of attack and sideslip
Normal, longitudinal, and transverse acceleration
Pitching angular velocity and acceleration
Rolling angular velocity and acceleration
Yawing angular velocity
Control positions

Shear, bending moment, and pitching moment on the right wing were measured by strain gages installed on the wing spars and skin at the wing root station 3 inches from the wing-fuselage junction as shown in figure 1. The outputs of the strain gages were recorded on a multichannel recording oscillograph. The data presented have been corrected for the inertia of the wing panel and are therefore the aerodynamic loads acting over the wing panel. Based on the results of a static calibration and an evaluation of the strain-gage response in flight, the estimated accuracies of the measured shear, bending moment, and pitching moment are ±100 pounds, ±400 foot-pounds, and ±200 foot-pounds, respectively.

In order to minimize the errors in total pressure measurements an NACA type A-6 total pressure head, described in reference 1, was mounted on the nose boom, and the static-pressure error was calibrated in flight. The estimated probable error in Mach number ranges from about ±0.01 near $M = 1.00$ to about ±0.03 at $M = 2.00$. The slightly higher probable error at the higher speeds is a direct function of the accuracy of the measurement of static pressure for the generally higher altitudes at which the maximum speeds are attained.

The accuracy of estimating the fuel consumed in rocket operations from fuel scheduling charts results in an estimated error of ±300 pounds in the weight determination. The estimated error in normal acceleration is of the order of ±0.02g. The airplane angle of attack was measured by a vane located on the nose boom and is presented herein as measured data.

## TESTS

The data presented were obtained during dives and accelerated maneuvers at altitudes from 40,000 to 70,000 feet over the Mach number

range from about 1.0 to 2.0. The Reynolds number for these tests varied from about $6 \times 10^6$ to $12 \times 10^6$ based on wing mean aerodynamic chord. The data were obtained with the airplane in a clean configuration with the wing leading-edge slats locked closed. Most of the data were obtained with no wing fences. However, for several flights the wing configuration included fences. Since no differences could be seen to exist between the data obtained with the wing fences on or off, the data are used interchangeably in this paper.

## RESULTS AND DISCUSSION

The aerodynamic characteristics of the D-558-II wing panel are presented in figure 3 for representative maneuvers at Mach numbers from 1.09 to 1.83. The data shown in figure 3 are presented as the variation of airplane normal-force coefficient, and right wing-panel normal-force, bending-moment, and pitching-moment coefficients with indicated angle of attack. Nonlinear variations are evident particularly in figures 3(a) and 3(b) at Mach numbers of 1.09 and 1.17, respectively, as reductions in the wing-panel normal-force and bending-moment-coefficient slopes and a change in the slope of the wing-panel pitching-moment curve. The reduction in wing-panel normal-force-coefficient slope is also apparent in the airplane normal-force-coefficient slope. These changes occur near angles of attack of $8^\circ$ and $11^\circ$ in figures 3(a) and 3(b), respectively. A reduction in the airplane longitudinal stability was experienced near these angles of attack as determined by the variation of elevator or stabilizer position with angle of attack and reported in reference 2.

At the higher Mach numbers (figs. 3(c) to 3(e)) the nonlinearities in the data are not as apparent and are evident primarily in the pitching-moment curves. At these Mach numbers it may be noted that the lift coefficients attained were not comparable to the lift coefficients where the change in slope occurred at the lower Mach numbers.

For comparison, wind-tunnel data showing the variation of the airplane normal-force coefficient with angle of attack obtained from references 3 and 4 for Mach numbers of 1.2 and 1.61 are shown on figures 3(b) and 3(d), respectively. The general trends of the flight and wind-tunnel data show good agreement, but a difference in the level of the flight-test and wind-tunnel data is apparent in figure 3(b).

At angles of attack below $8^\circ$ and $11^\circ$ in figures 3(a) and 3(b), respectively, and over the entire lift range investigated at the higher Mach numbers the wing-panel and airplane normal-force curves are essentially linear. The wing-panel and airplane normal-force-curve slopes were therefore obtained for the linear region by taking slopes of the

data of figure 3, and are presented in figure 4 as the variation of airplane and wing-panel normal-force-curve slopes with Mach number. Both the wing-panel and airplane normal-force-curve slopes decrease from a value of about 0.088 at a Mach number of 1.10 to a value of about 0.050 at a Mach number of 1.85.

The wing-panel data of figure 3 are presented in figure 5 as the variation of wing-panel bending-moment, and pitching-moment coefficients with wing-panel normal-force coefficient. Also shown on this figure is the variation of the wing-panel lateral and chordwise center of pressure with wing-panel normal-force coefficient. The spanwise and chordwise center-of-pressure locations are not shown at wing-panel normal-force coefficients below 0.2 at a Mach number of 1.83 since their location becomes meaningless at normal-force coefficients approaching zero. For reference, the value of wing-panel normal-force coefficient corresponding to angles of attack of 8° and 11° are indicated on figures 5(a) and 5(b), respectively, by the vertical lines above the curves. At these angles of attack a reduction in the wing-panel bending-moment-coefficient slope occurs associated with an inboard movement of the lateral center of pressure. The pitching-moment curve changes to an unstable slope associated with a small forward movement of the chordwise center of pressure. At even higher lifts the pitching-moment curves change to a stable slope associated with a small rearward movement of the chordwise center of pressure, and an apparent increase in the slope of the bending-moment curve occurs caused by a small outboard movement of the lateral center of pressure. At the higher Mach numbers the data are essentially linear with small variations in the pitching-moment-coefficient curves.

For comparable lift ranges the center-of-pressure movement with changes in Mach number is small. The spanwise center of pressure is located at about 39 percent of the wing-panel semispan and the chordwise center of pressure is located at about 33 percent of the wing-panel mean aerodynamic chord over the speed range of these tests.

The small changes with Mach number are also illustrated in figure 6 where the wing-panel normal-force, bending-moment, and pitching-moment coefficients are presented as variations with Mach number for constant airplane normal-force coefficients of 0.25 and 0.60 over the Mach number range from 1.0 to 2.0. At the higher Mach numbers the pitching-moment-coefficient data are not available.

## CONCLUDING REMARKS

Measurements of the wing loads on the D-558-II airplane over the supersonic Mach number range from 1.0 to 2.0 have indicated nonlinear variations of the wing characteristics with angle of attack. These

nonlinear characteristics were apparent primarily at the lower supersonic speeds as a reduction in the wing-panel normal-force-curve slope, and an inboard and forward movement of the center of pressure at the higher lifts. At the higher Mach numbers, where a smaller lift range was investigated, the nonlinearities were apparent primarily in the pitching-moment curves.

For comparable lift ranges the changes in the wing characteristics with Mach number were small.

High-Speed Flight Station,
National Advisory Committee for Aeronautics,
Edwards, Calif., December 23, 1954.

## REFERENCES

1. Gracey, William, Coletti, Donald E., and Russell, Walter R.: Wind-Tunnel Investigation of a Number of Total-Pressure Tubes at High Angles of Attack - Supersonic Speeds. NACA TN 2661, 1951.

2. Ankenbruck, Herman O.: Determination of Longitudinal Stability in Supersonic Accelerated Maneuvers for the Douglas D-558-II Research Airplane. NACA RM L53J20, 1954.

3. Osborne, Robert S.: High-Speed Wind-Tunnel Investigation of the Longitudinal Stability and Control Characteristics of a 1/16-Scale Model of the D-558-II Research Airplane at High Subsonic Mach Numbers and at a Mach Number of 1.2. NACA RM L9C04, 1949.

4. Spearman, M. Leroy: Static Longitudinal Stability and Control Characteristics of a 1/16-Scale Model of the Douglas D-558-II Research Airplane at Mach Numbers of 1.61 and 2.01. NACA RM L53I22, 1953.

TABLE I

PHYSICAL CHARACTERISTICS OF THE DOUGLAS D-558-II AIRPLANE

| | |
|---|---|
| **Wing:** | |
| Root airfoil section (normal to 0.30 chord of unswept panel) | NACA 63-010 |
| Tip airfoil section (normal to 0.30 chord of unswept panel) | NACA $63_1$-012 |
| Total area, sq ft | 175.0 |
| Span, ft | 25.0 |
| Mean aerodynamic chord, in. | 87.301 |
| Root chord (parallel to plane of symmetry), in. | 108.51 |
| Extended tip chord (parallel to plane of symmetry), in. | 61.18 |
| Taper ratio | 0.565 |
| Aspect ratio | 3.570 |
| Sweep at 0.30 chord of unswept panel, deg | 35.0 |
| Sweep of leading edge, deg | 38.8 |
| Incidence at fuselage center line, deg | 3.0 |
| Dihedral, deg | -3.0 |
| Geometric twist, deg | 0 |
| Total aileron area (rearward of hinge line), sq ft | 9.8 |
| Aileron travel (each), deg | ±15 |
| Total flap area, sq ft | 12.58 |
| Flap travel, deg | 50 |
| **Wing panel:** | |
| Area, sq ft | 127.6 |
| Span, ft | 19.5 |
| Mean aerodynamic chord, in. | 81.334 |
| **Horizontal tail:** | |
| Root airfoil section (normal to 0.30 chord of unswept panel) | NACA 63-010 |
| Tip airfoil section (normal to 0.30 chord of unswept panel) | NACA 63-010 |
| Total area, sq ft | 39.9 |
| Span, in. | 143.6 |
| Mean aerodynamic chord, in. | 41.75 |
| Root chord (parallel to plane of symmetry), in. | 53.6 |
| Extended tip chord (parallel to plane of symmetry), in. | 26.8 |
| Taper ratio | 0.50 |
| Aspect ratio | 3.59 |
| Sweep at 0.30 chord line of unswept panel, deg | 40.0 |
| Dihedral, deg | 0 |

TABLE I.- Concluded

PHYSICAL CHARACTERISTICS OF THE DOUGLAS D-558-II AIRPLANE

| | |
|---|---|
| Elevator area, sq ft | 9.4 |
| Elevator travel, deg | |
| Up | 25 |
| Down | 15 |
| Stabilizer travel, deg | |
| Leading edge up | 4 |
| Leading edge down | 5 |
| **Vertical tail:** | |
| Airfoil section (normal to 0.30 chord of unswept panel) | NACA 63-010 |
| Effective area (area above root chord), sq ft | 36.6 |
| Height from fuselage reference line, in. | 98.0 |
| Root chord (chord 24 in. above fuselage reference line), in. | 116.8 |
| Extended tip chord (parallel to fuselage reference line), in. | 27.0 |
| Sweep angle at 0.30 chord of unswept panel, deg | 49.0 |
| Rudder area (aft hinge line), sq ft | 6.15 |
| Rudder travel, deg | ±25 |
| **Fuselage:** | |
| Length, ft | 42.0 |
| Maximum diameter, in. | 60.0 |
| Fineness ratio | 8.40 |
| Speed-retarder area, sq ft | 5.25 |
| **Power plant:** | |
| Rocket | LR8-RM-6 |
| **Airplane weight, lb:** | |
| Full rocket fuel | 15,787 |
| No fuel | 9,421 |
| **Center-of-gravity locations, percent M.A.C.:** | |
| Full rocket fuel (gear up) | 24.6 |
| No fuel (gear up) | 27.3 |
| No fuel (gear down) | 26.7 |

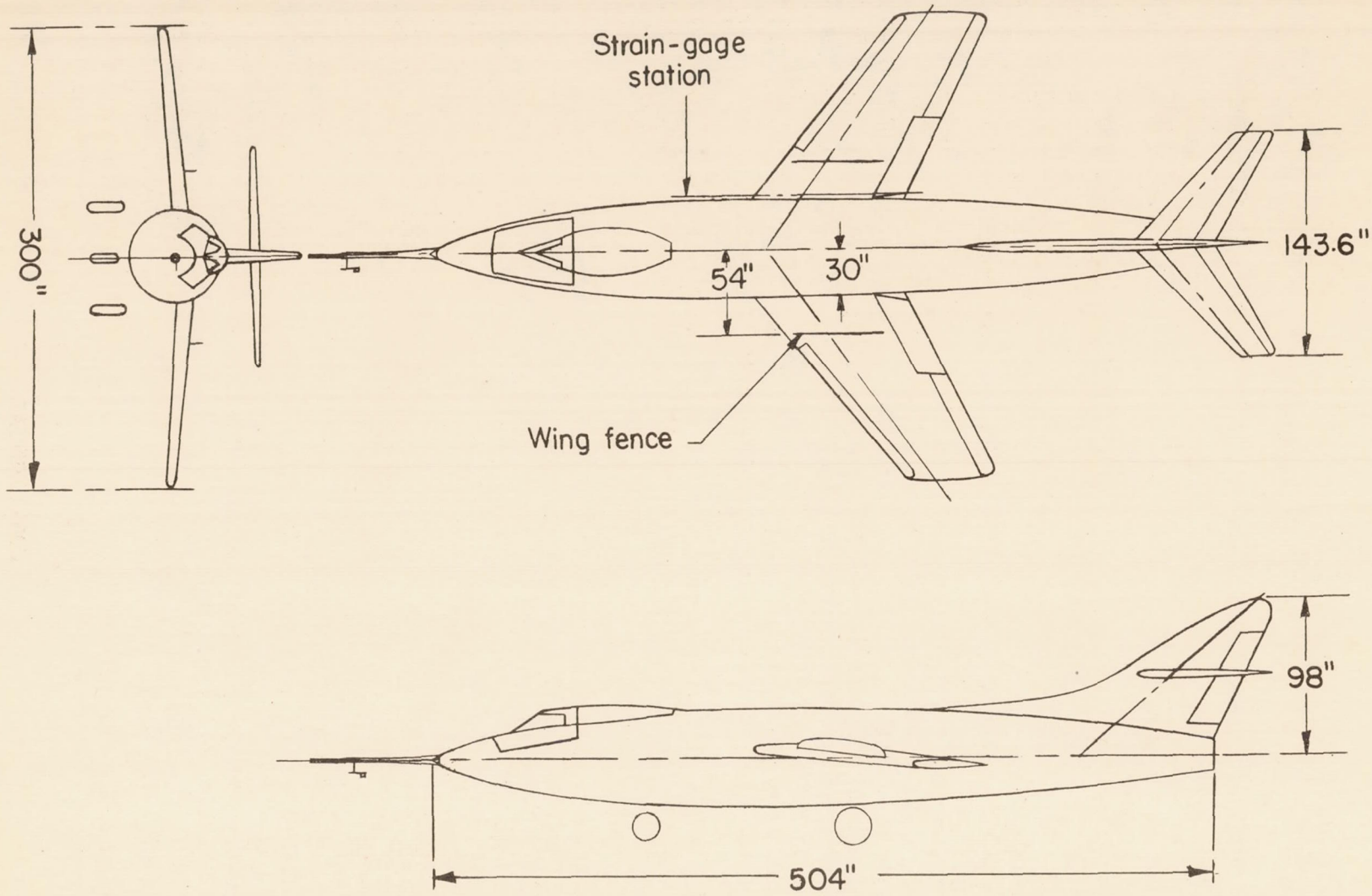


Figure 1.- Three-view drawing of the Douglas D-558-II research airplane.

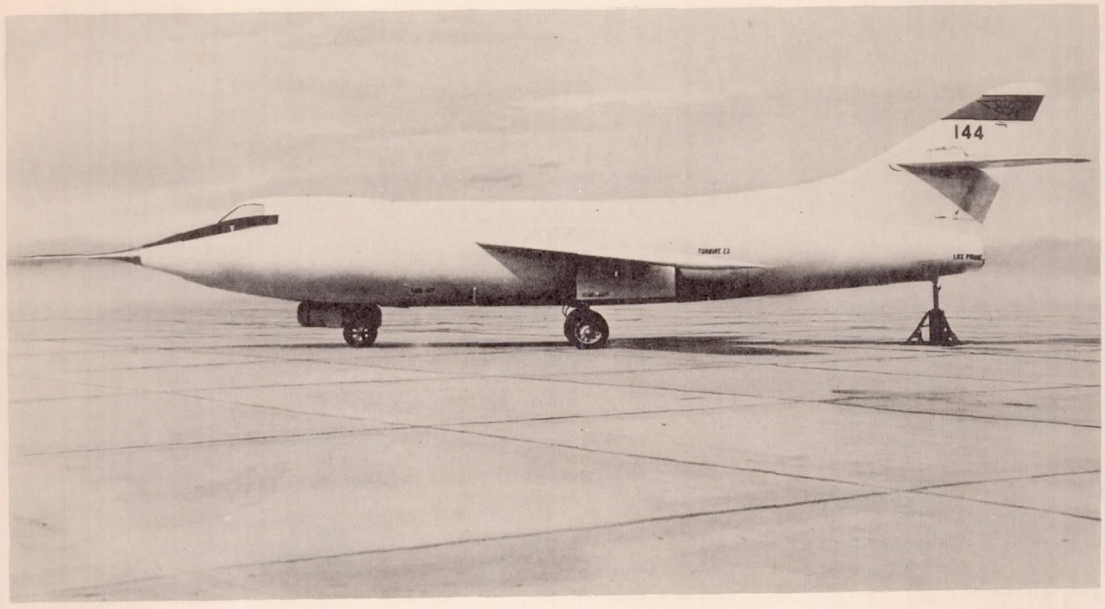


L-73284

(a) Side view.

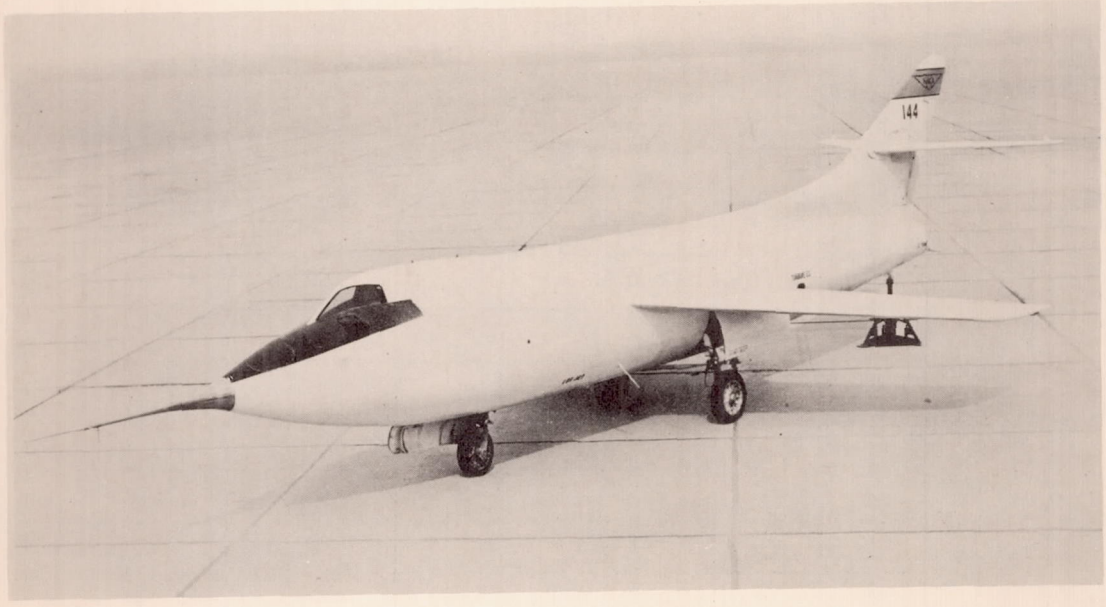


L-73282

(b) Three-quarter front view.

Figure 2.- Photographs of the Douglas D-558-II research airplane.

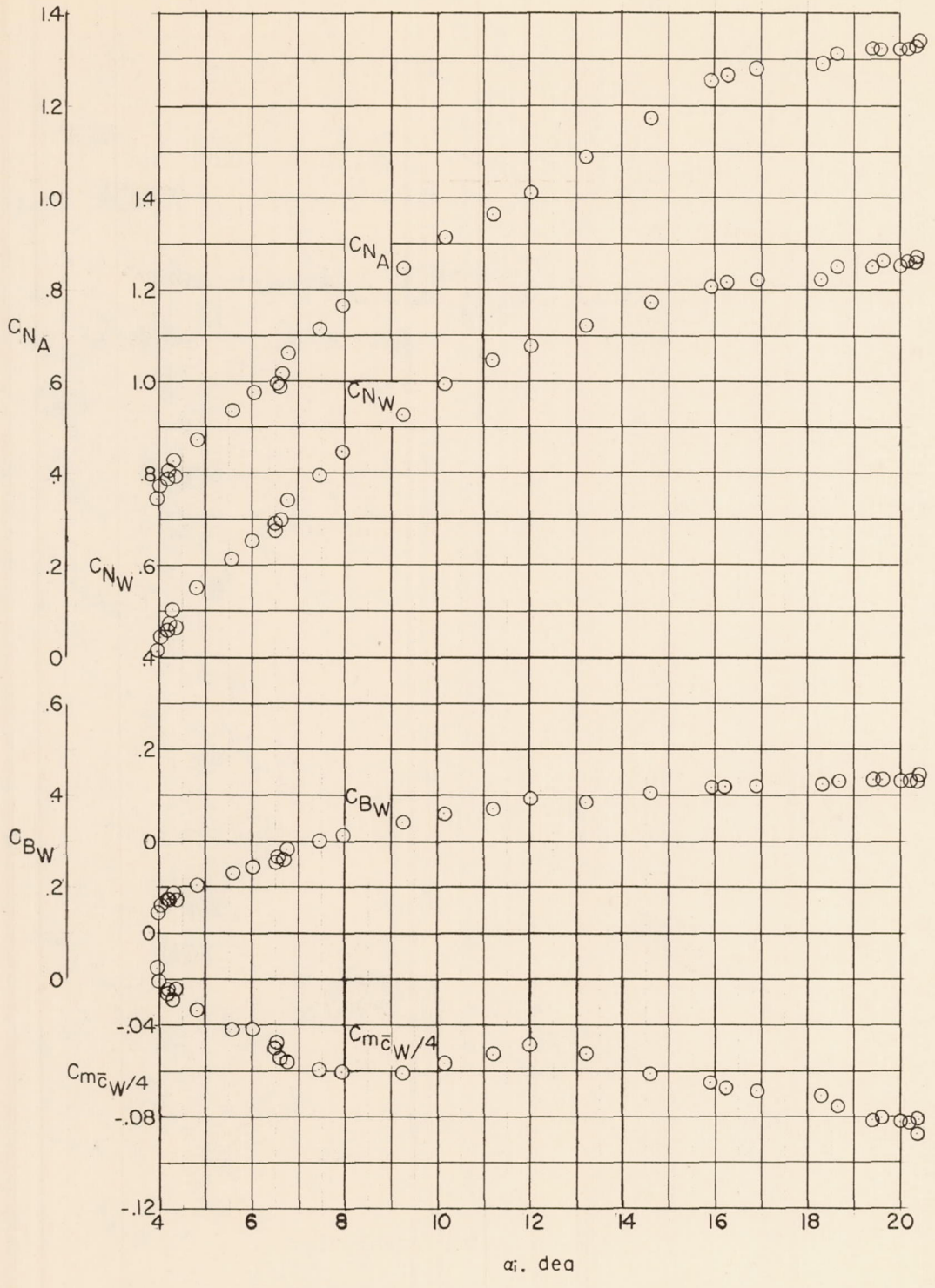


(a) M = 1.09; $h_p$ = 46,300 feet.

Figure 3.- Variation of airplane normal-force coefficient and wing-panel characteristics with angle of attack during wind-up turns.

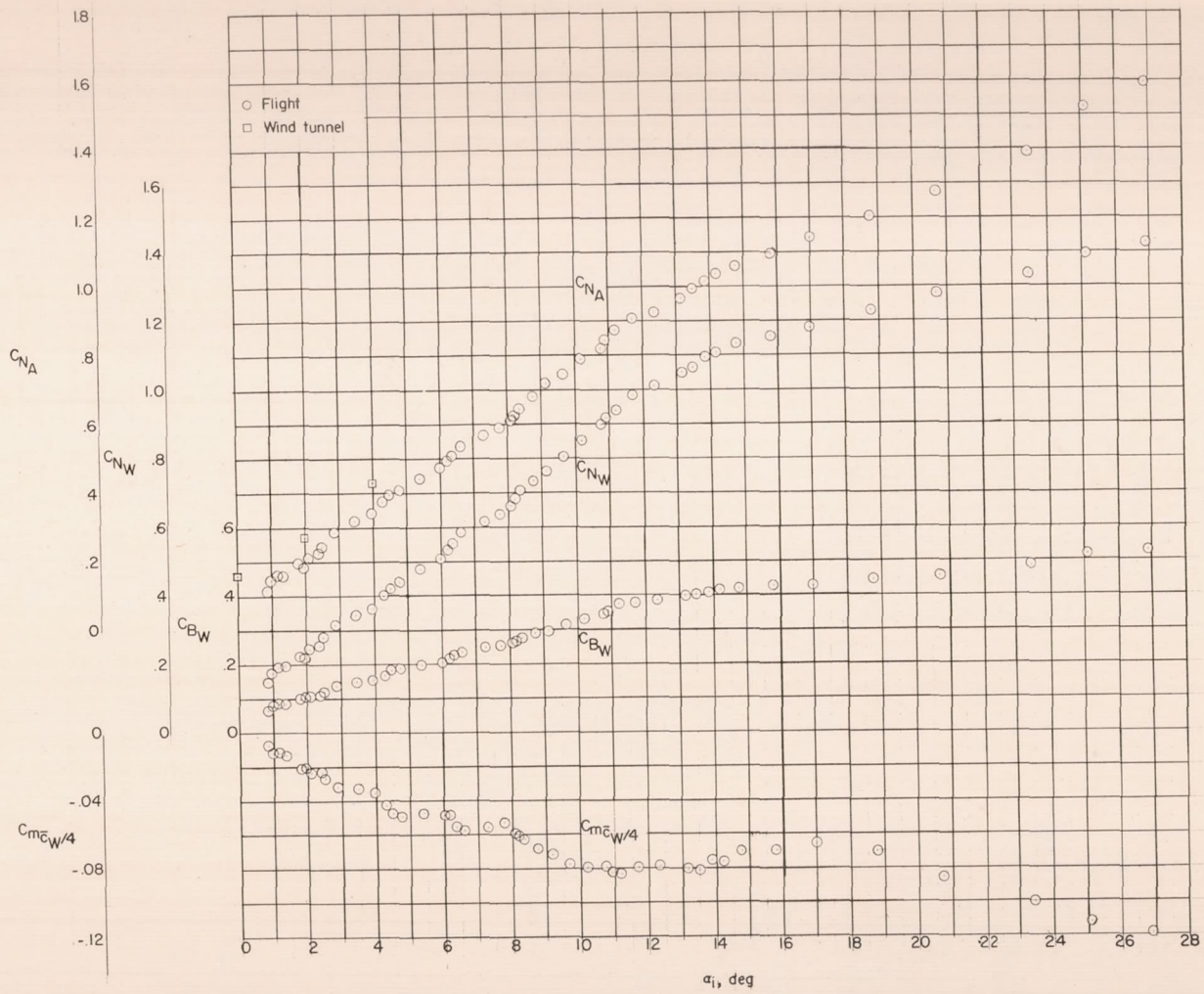


(b) M = 1.17; $h_p$ = 52,000 feet.

Figure 3.- Continued.

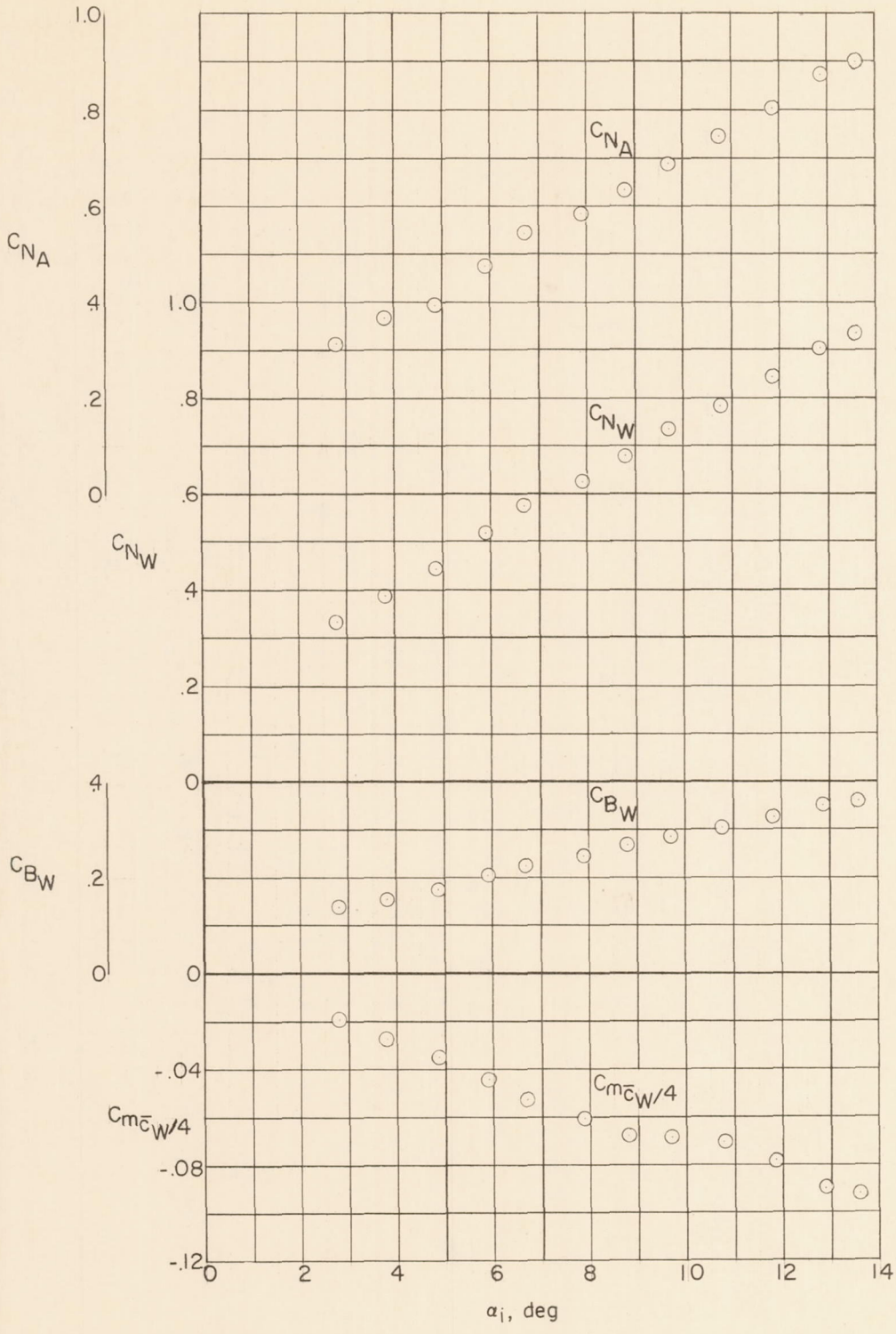


(c) M = 1.38; $h_p$ = 64,000 feet.

Figure 3.- Continued.

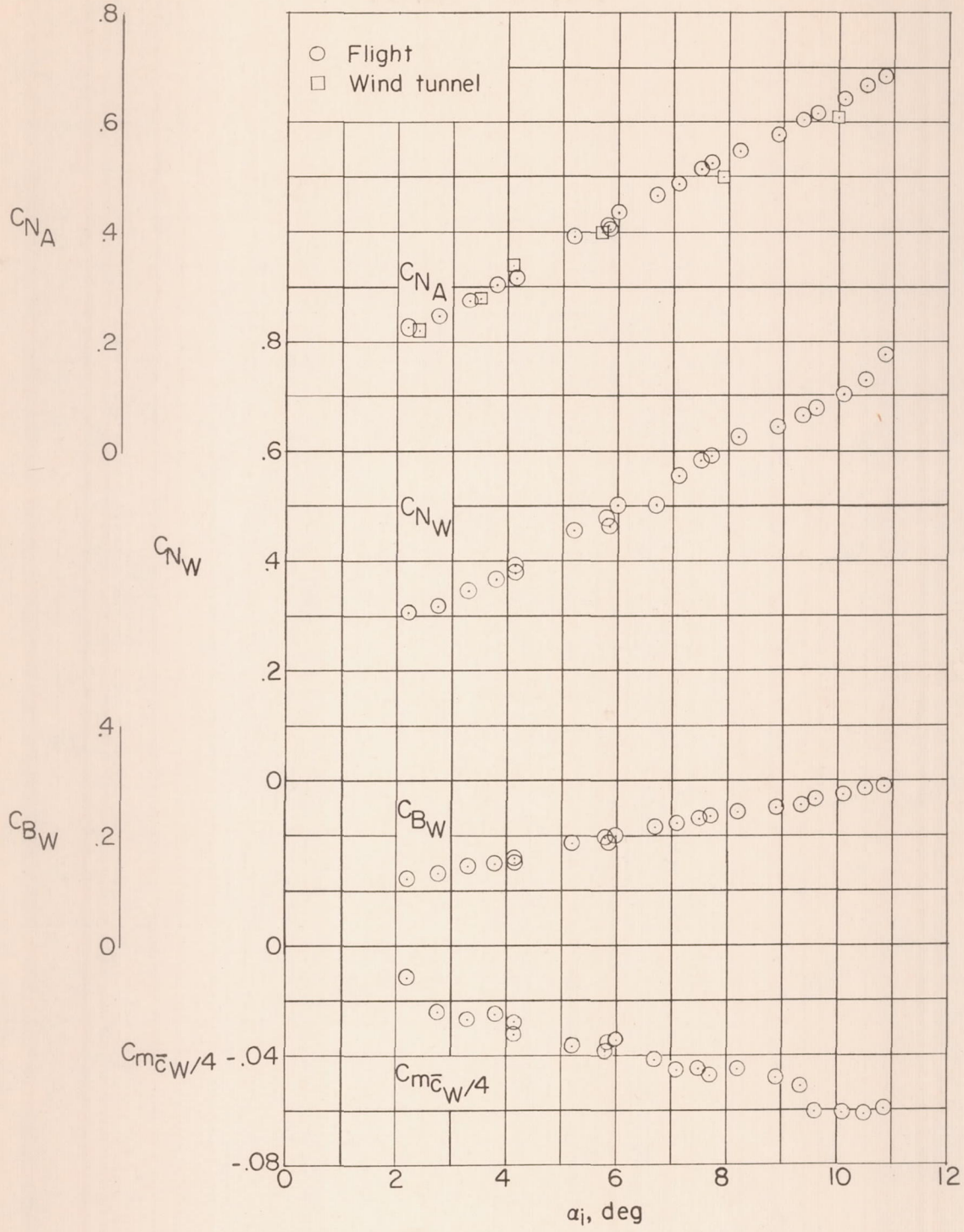


(d) M = 1.57; $h_p$ = 61,000 feet.

Figure 3.- Continued.

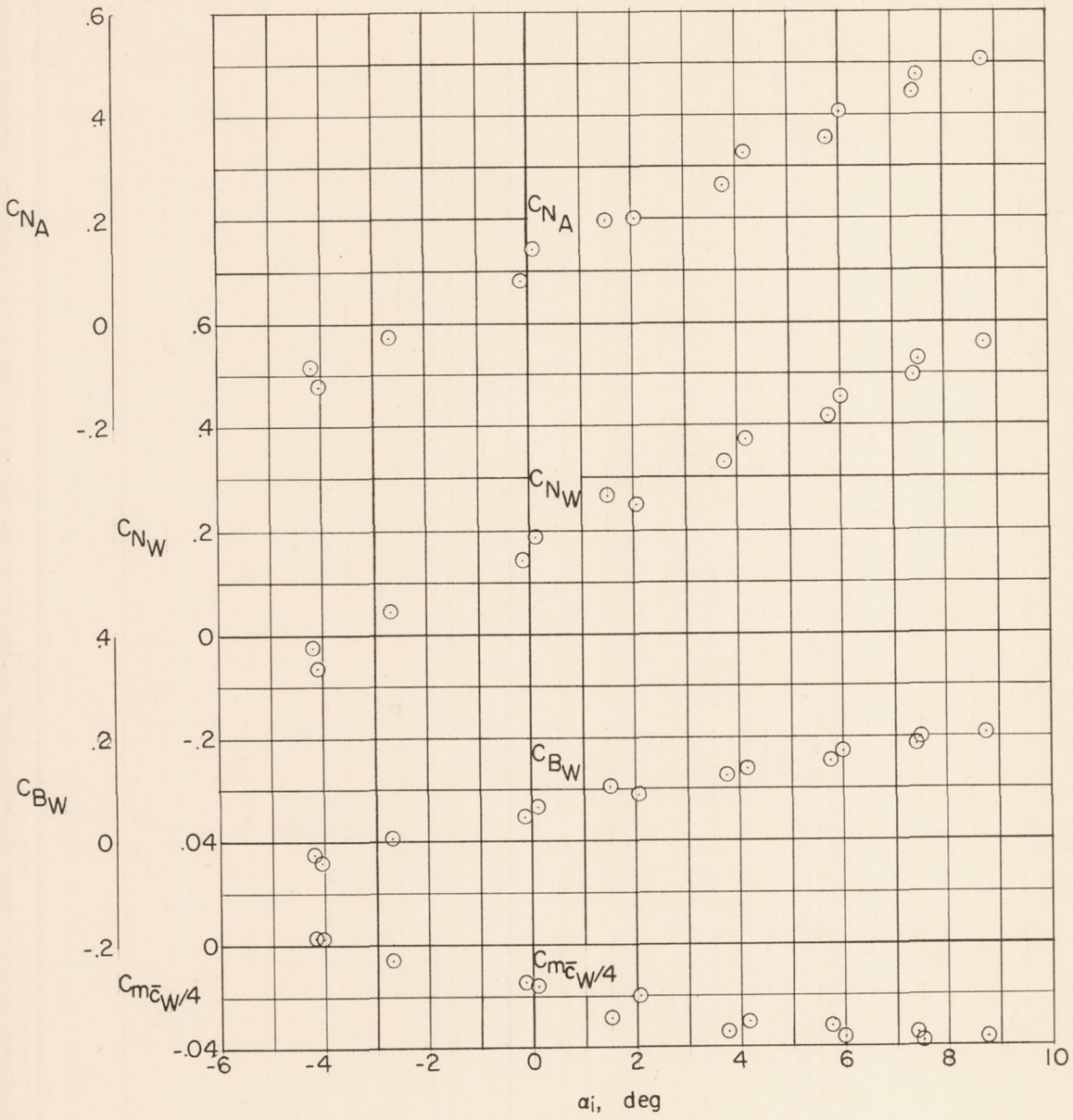


(e) M = 1.83; $h_p$ = 66,000 feet.

Figure 3.- Concluded.

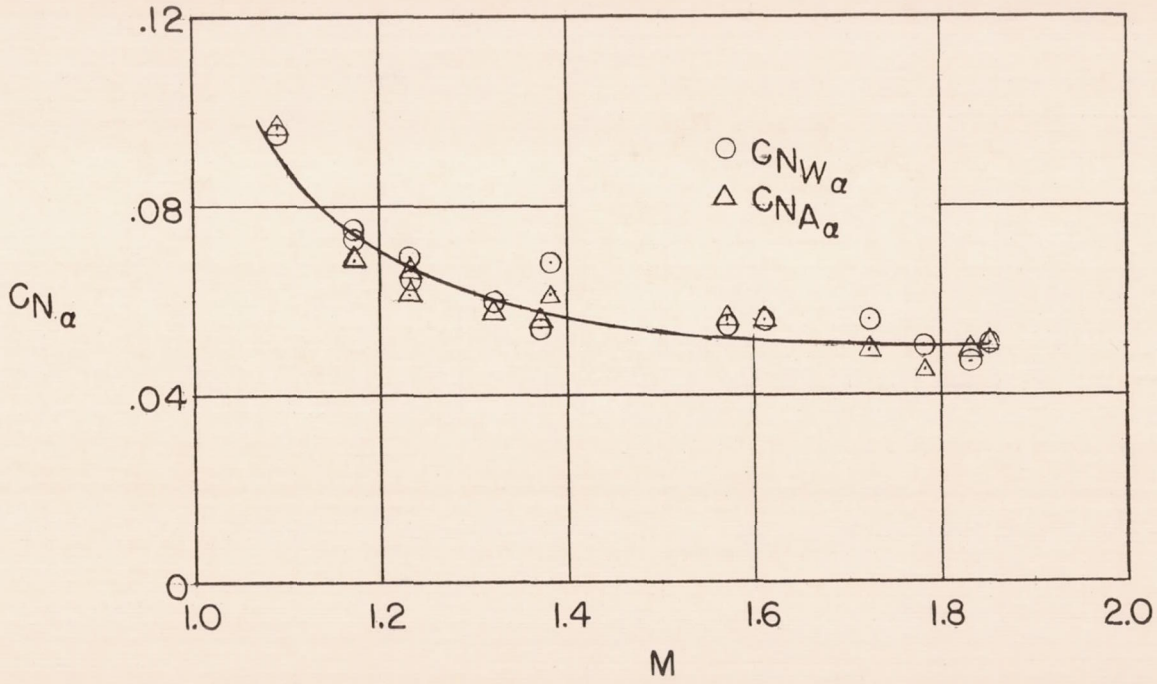


Figure 4.- Variation of airplane and wing-panel normal-force curve slope with Mach number.

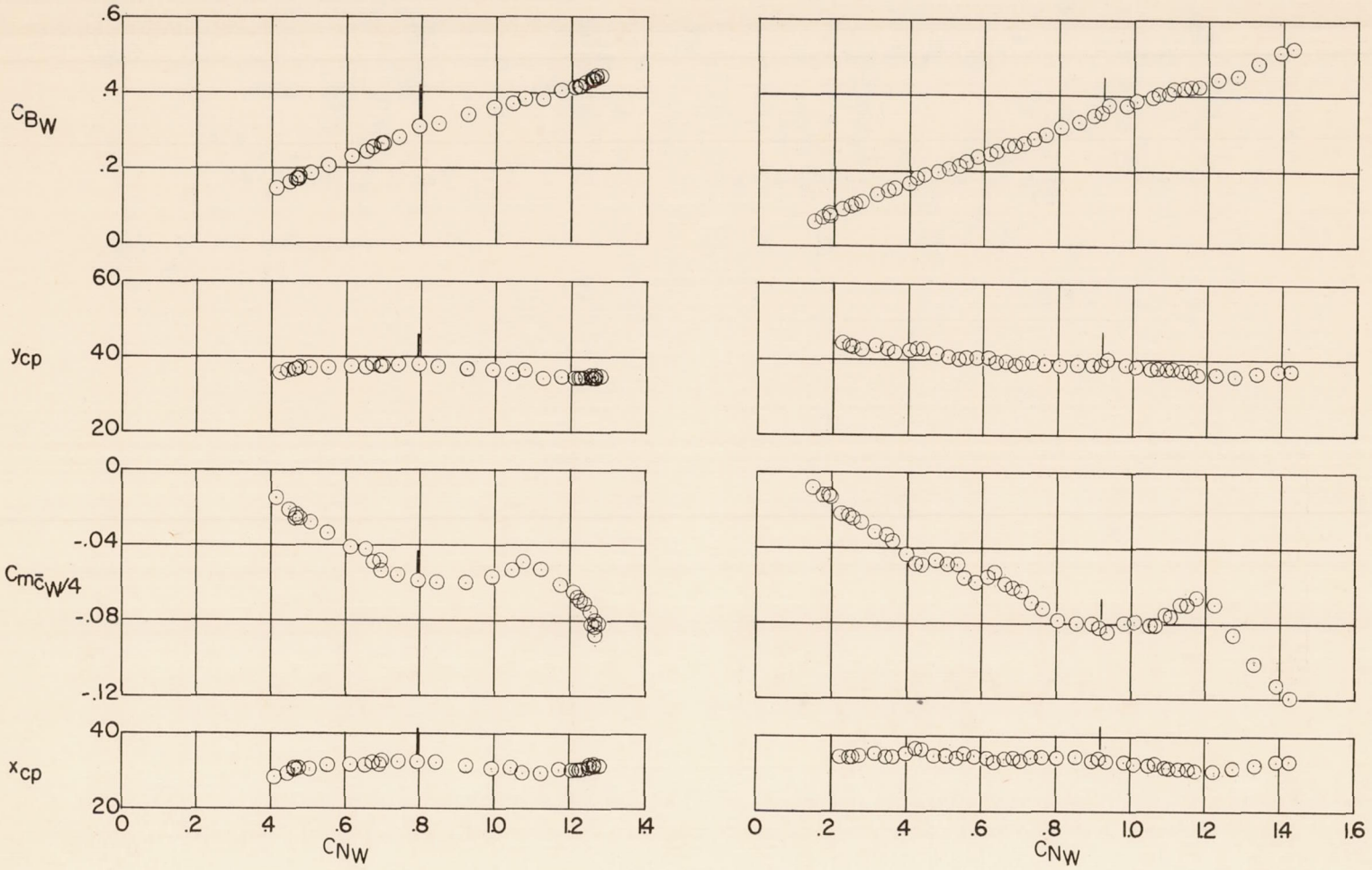


(a) M = 1.09. (b) M = 1.17.

Figure 5.- Variation of wing-panel bending-moment coefficient, spanwise center of pressure, wing-panel pitching-moment coefficient and chordwise center of pressure with wing-panel normal-force coefficient.

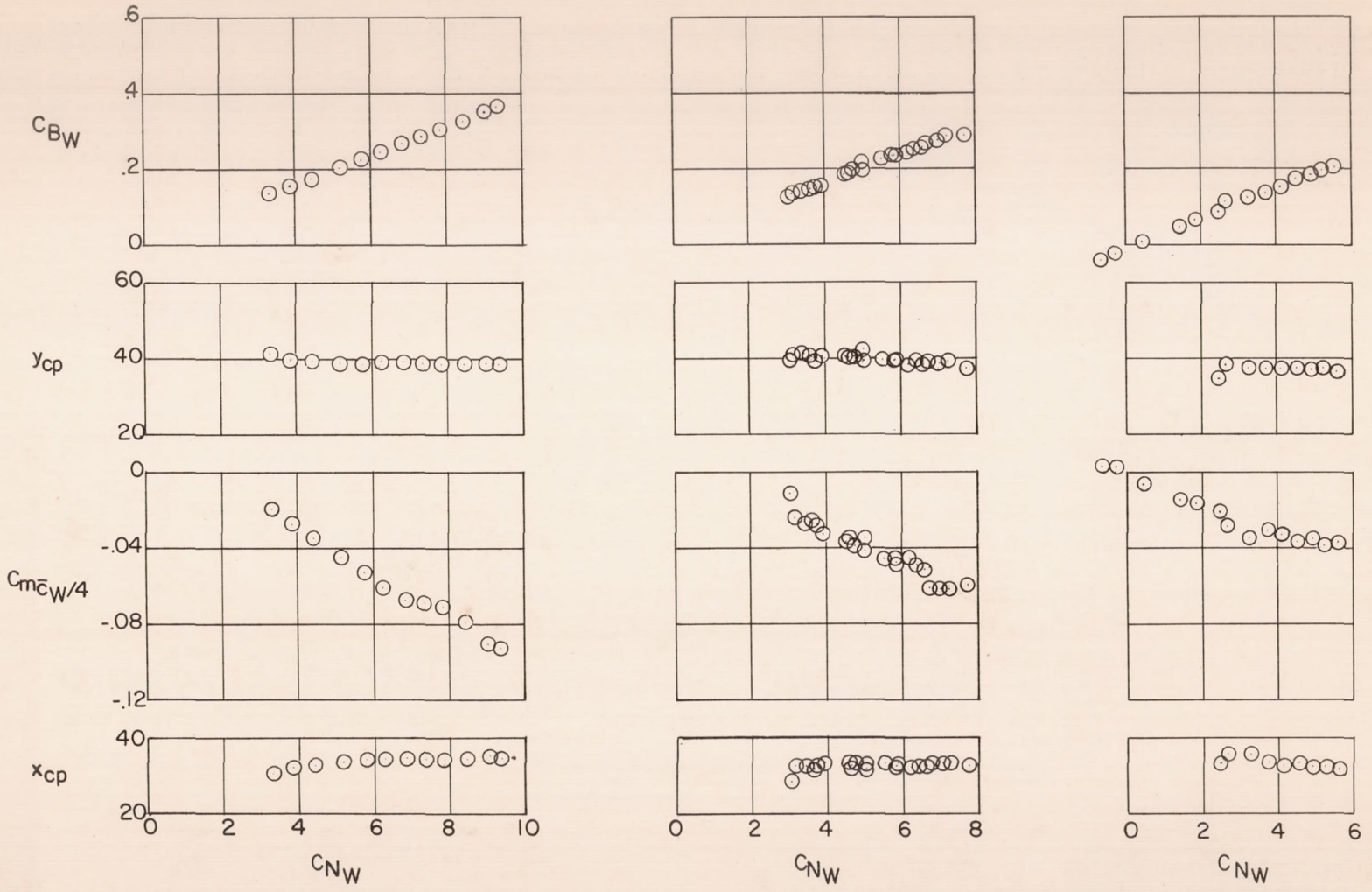


(c) M = 1.38. (d) M = 1.57. (e) M = 1.83.

Figure 5.- Concluded.

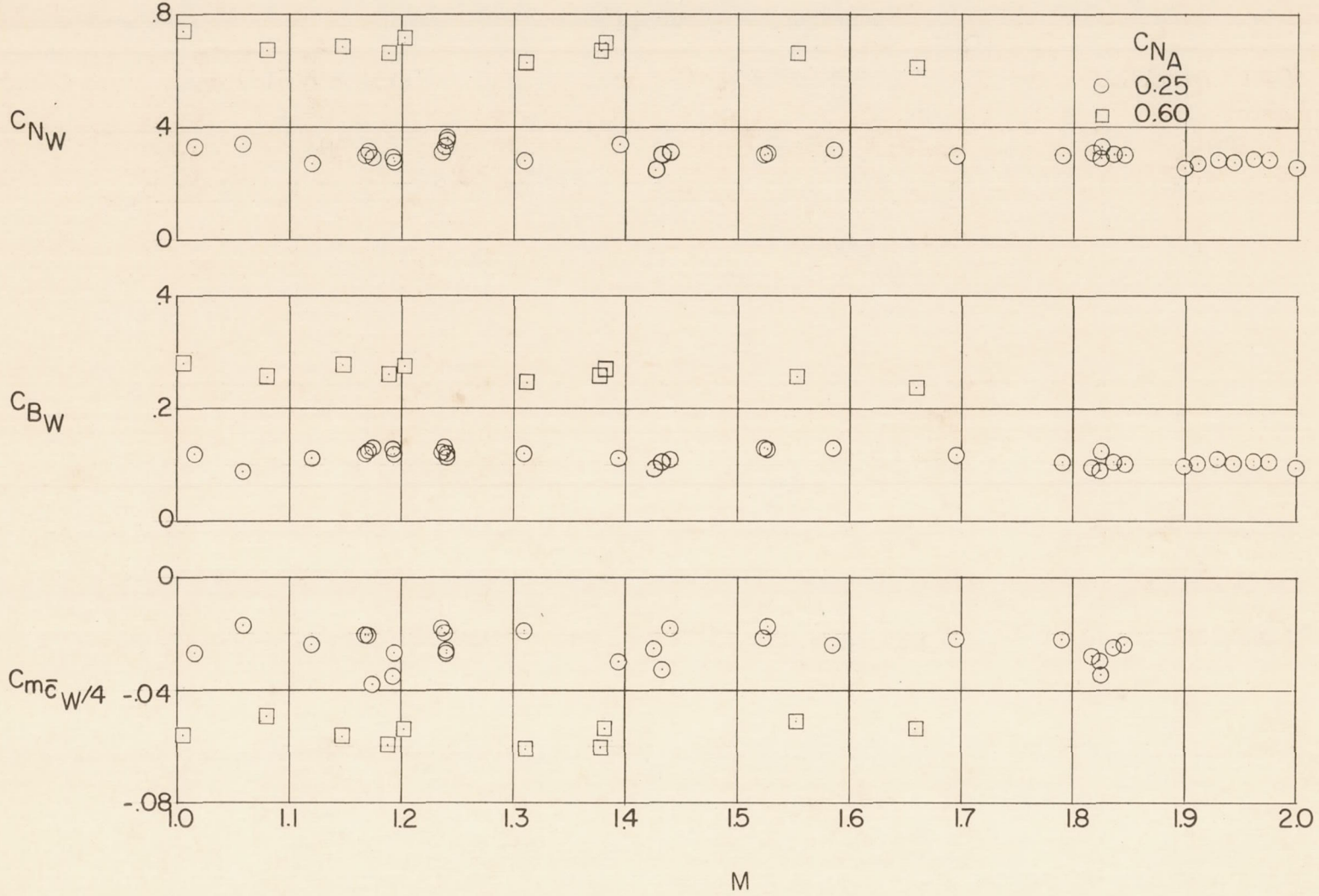


Figure 6.- Variation of wing-panel normal-force, bending-moment and pitching-moment coefficients with Mach number for airplane normal-force coefficients of 0.25 and 0.60.